ELSEVIER

www.elsevier.nl/locate/jorganchem

Journal of Organometallic Chemistry 588 (1999) 42–50

Journal of Organometallic Chemistry

Solid state, structural and solution studies on bis(2-methylbenzyl)-selenide, methyl(2,4,6-tri-*t*-butylphenyl)-selenide, bis(2,4,6-tri-methylphenyl)-diselenide, and bis(2,4,6-tri-*t*-butylphenyl)-diselenide

Paul M. Dickson, Margaret A.D. McGowan, Burl Yearwood, Mary Jane Heeg, John P. Oliver *

Department of Chemistry, Wayne State University, Detroit, MI 48202, USA

Received 11 February 1999

Abstract

Two selenides, $(2\text{-MeBz})_2Se$ (**1**) and MeMes*Se (**2**) and two diselenides, Mes_2Se_2 (**3**) and $Mes^*_2Se_2$ (**4**) have been prepared and characterized by single-crystal X-ray diffraction and by NMR spectroscopy. The structure of **1** was solved in the orthorhombic space group *Pbca* (no. 61) with cell constants $a = b = 13.944(10)$ Å, $c = 14.30(2)$ Å. The structure of **2** was determined in space group $P\bar{1}$ (no. 2) with cell constants $a = 5.9443(5)$ Å, $b = 18.665(2)$ Å, $c = 26.372(3)$ Å, $\alpha = 99.393(2)°$, $\beta = 90.890(2)°$ and $\gamma = 92.703(2)°$. The structures of **3** and **4** were determined in the monoclinic space group $P2_1/c$ (no. 14) with unit cell parameters for **3** of $a = 6.333(1)$ Å, $b = 18.370(4)$ Å, $c = 5.122(3)$ Å, $\beta = 97.42(3)°$ and for **4**, $a = 11.359(5)$ Å, $b = 10.520(8)$ Å, $c = 30.22(2)$ Å and $\beta = 98.94(4)°$. A rotational process has been studied in **4** and the kinetics and thermodynamic parameters for this process are determined from DNMR measurements using three different methods, measurement of coalescence temperatures, calculation of kinetic parameters using the line half-width approximation, and by full line shape analysis. The results from these three methods were compared.

Keywords: Selenium; Structure; Kinetics; Mechanism; Rotational barrier; NMR

1. Introduction

Our interest in the reactions of the higher chalcogens, S, Se, and Te, and their organic derivatives with Group 13 organometallic species necessitated the preparation and characterization of a number of organoselenides and -diselenides. In this paper we report the syntheses and structures of two selenides and two aryl diselenides, their characterization by NMR spectroscopy and by X-ray diffraction.

A large number of organoselenides and diselenides have been prepared, but only a few have been well characterized by modern spectroscopic and structural methods. The structures of diselenides with different substituents have been reported [1–11], and from these studies, it has been suggested that diselenides relieve steric strain by increasing the dihedral angle about the Se–Se bond rather than by increasing the Se–Se and Se–C bond lengths [3]. The effect of changing the dihedral angle on UV spectra also has been examined [3]. The substituent bound to the Se or Se_2 moiety alters the ^{77}Se chemical shift [12], and with very bulky substituents present on the diselenides, gives rise to a slow rotational process [13]. In this paper, we offer further proof that this is the case by examining the crystal structures of Mes_2Se_2, **3**, and $Mes^*_2Se_2$, **4** (Mes = 2,4,6-trimethylphenyl; Mes* = 2,4,6-tri-*t*-butylphenyl). It also will be seen that, in the case of **4**, not all of the strain is relieved by this increase in dihedral angle but is manifested in other structural distortions. The dise-

* Corresponding author.

PII: S0022-328X(99)00343-5

lenides were characterized by ^{1}H-, ^{13}C-, ^{77}Se-, and variable-temperature ^{1}H-NMR in order to probe the structure of the compounds in solution and to reexamine the barrier to rotation about the Se–Se bond in **4** first reported by Kessler and Rundel [13]. The structure of the first symmetric alkyl selenide, bis(2-methylbenzyl)selenide, **1**, is described.

2. Experimental

2.1. General experimental procedures

All manipulations were performed in the absence of water and air using standard Schlenk line and dry box techniques [14], but the final products are air-stable. They are, however, toxic and have a very strong stench, so they should be kept in sealed containers at all times. Argon was purified by passing it through a series of columns containing Deox catalyst (Alfa), calcium sulfate, and phosphorus pentoxide. All solvents used were dried using standard techniques, and all glassware was oven-dried. 2-Bromomesitylene (Aldrich) and 2-methylbenzyl chloride (Lancaster) were used as received. 1-Bromo-2,4,6-tri-*t*-butylbenzene was synthesized according to published procedures [15]. ^{1}H- and ^{13}C-NMR spectra were recorded on either a Gemini-300 or a Varian-U500 NMR spectrometer. The chemical shifts were referenced to the residual proton line from benzene-d_6 ($\delta = 7.15$ ppm for ^{1}H; $\delta = 128.0$ for ^{13}C). ^{77}Se-NMR were obtained at 20°C in C_6D_6 on a Varian-U500 spectrometer at 95.349 MHz and were referenced to an external standard of Me_2Se_2 (2.48 M solution in C_6D_6 270 ppm). Variable-temperature NMR spectra were obtained on GN-300 and U-500 spectrometers on a 0.077 M solution of **4** in $CDCl_3$ over a 120°C range (-60 to $+60$°C). The syntheses of **3** and **4** were modified from the literature procedures for the synthesis of the disulfides [16,17] and diselenides [18,19]. Other procedures can be found in the paper by du Mont et al. [20] and references therein.

2.2. Synthesis of (2-MeBz)$_2$Se (1)

A solution of 2-methylbenzyl magnesium chloride (0.056 mol in 200 ml of ether) was added dropwise to a suspension of 4.45 g (0.056 mol) of selenium in 150 ml of ether. The mixture was maintained at reflux for 12 h, yielding the 2-methylbenzylseleno Grignard reagent. At this point 5.9 ml (0.045 mol) of 2-methylbenzyl chloride was added dropwise to the resulting colorless solution which was stirred for about an hour during which time a precipitate of magnesium chloride formed. The resulting colorless solution was decanted from the remaining selenium; the volume of solvent was reduced and placed in the freezer (-30°C) to crystallize. Colorless crystals of **1** were obtained in quantitative yield. m.p. 74–76°C; ^{1}H-NMR (C_6D_6) δ 2.072 (s, 3H, CH_3), 3.466 (s, 2H, CH_2), 7.05–6.90 (m, 4H, C_6H_4); ^{13}C {^{1}H}(C_6D_6) 26.2 (s, *C*H_3), δ 66.4 (*C*H_2), δ 122–141 (C_6H_4).

2.3. Preparation of MeMes*Se (2)

MeMes*Se, **2**, was obtained as a product in the preparation of $Me_2InSeMes^*$. Bis(2,4,6-tri-*t*-butylphenyl) diselenide (8.26 g, 0.0127 mol) was added dropwise from a syringe to a solution of $Me_3In{\cdot}OEt_2$ (40 ml, 0.212 mol) in 60 ml of hexane. The orange color of the diselenide disappeared on addition to the trimethylindium. The mixture was stirred for 2 days at room temperature. A yellow precipitate was formed. The solvent was removed by vacuum to yield both colorless and yellow crystals. NMR analysis shows the yellow crystals are the same as the colorless crystals except coated with a yellow diselenide layer. The $Me_2InSeMes^*$ product was removed with the solvent and yielded no crystals. The colorless crystals of **2** were used for diffraction studies. Yield 60% (yellow/colorless crystals). m.p. 190–192°C; ^{1}H-NMR (C_6D_6; δ, ppm): 1.24 (s, 9H, *p*-C(CH_3)$_3$ of Mes*), 1.31 (s, 18H, *o*-C(CH_3)$_3$ of Mes*), 1.37 (s, 3H, CH_3–Se), 7.38 (s, 2H, aryl of Mes*). ^{13}C {^{1}H} (C_6D_6; δ, ppm): 31.44 (*p*-C(*C*H_3)$_3$), 31.78 (*C*H_3–Se), 32.86 (*o*-C(*C*H_3)$_3$), 33.11 (*p*-*t*-Bu), 38.97 (*o*-*t*-Bu), 122.71 (*C*H), 150.51 (*p*-*C*-*t*-Bu).

2.4. Synthesis of Mes$_2$Se$_2$ (3)

A total of 5 g (25.1 mmol) of 2-bromomesitylene was added to 0.74 g (30 mmol) of Mg in 200 ml of ethyl ether and maintained at reflux until all of the bromide had reacted (about 8 h). The solution was decanted into a three-necked flask equipped with an argon inlet, a condenser, and a bent side arm containing 1.98 g (25 mmol) of gray selenium. The selenium was added over a period of 6 h in small portions by slowly tipping up the side arm. This yellowish solution was decanted from any unreacted selenium and cooled to 0°C. To this solution was added 10 ml concentrated HCl and then oxygen was bubbled through the solution to afford the bright orange, foul-smelling diselenide which was extracted with ether. X-ray-quality crystals were obtained by recrystallization from toluene at ambient temperature. Yield 90%. ^{1}H-NMR in C_6D_6 1.990 (s, 3H, *p*-CH_3), 2.281 (s, 6H, 2,6-CH_3), 6.636 (s, 2H, C_6H_2); ^{13}C{^{1}H} 20.62 (*p*-CH_3), 24.06 (2,6-CH_3), 128.38 (*C*H), 128.98 (*C*–Se), 138.83 (*p*-*C*–Me), 143.53 (2,6-*C*–Me); ^{77}Se{^{1}H} 0.16 M solution in C_6D_6 at 21°C 368 ppm.

2.5. Synthesis of $Mes^*_2Se_2$ (4)

A total of 3 g (9.2 mmol) of 1-bromo-2,4,6-tri-*t*-butylbenzene was added to 0.22 g (9.2 mmol) of Mg in 200 ml of THF and maintained at reflux until all of the Mg had reacted (about 20 h). The solution was decanted to a three-necked flask equipped with an argon inlet, a condenser, and a side arm containing 0.72 g (9.1 mmol) of gray selenium which was added over a period of 6 h in small portions. This yellowish solution was decanted from any unreacted selenium and cooled to 0°C. To this solution was added 10 ml concentrated HCl and then oxygen was bubbled through the solution to afford the bright orange, foul-smelling diselenide which was extracted with THF. X-ray-quality crystals were obtained by recrystallization from toluene at ambient temperature. Yield 50%. ^{1}H- and ^{13}C-NMR are similar to those reported by du Mont [20]. ^{1}H-NMR in C_6D_6 1.248 (s, 9H, *p*-C(CH_3)$_3$), 1.428 (broad s, 18H, 2,6-C(CH_3)$_3$), 7.381 (broad s, 2H, C_6H_2); ^{13}C{^{1}H} 31.43 (*p*-C(CH_3)$_3$), 33.50 (2,6-C(CH_3)$_3$), 35.05 (*p*-*C*(CH_3)$_3$), 39.30 (2,6-*C*(CH_3)$_3$), 122.64 (*C*H), 150.45 (*p*-*C*-*t*-Bu), 156.48 (2,6-*C*-*t*-Bu); ^{77}Se{H} 0.077 M solution in C_6D_6 at 21°C 521 ppm.

3. Crystallographic experimental

Crystals of **1**–**4** were grown as described in Section 2. In each case, a suitable crystal was glued to the end of a glass fiber or sealed in a thin-walled capillary tube, and mounted on a goniometer head. **1**, **3** and **4** were placed on a Nicolet $P2_1$ diffractometer for data collection. Data reduction was carried out using SHELXTL-PC [21]. Data for **2** were collected at room temperature on a Siemens P4/CCD SMART system [22]. A total of 1390 frames was collected at a distance of 5 cm at 10 s frame^{-1} yielding 14 558 integrated reflections. Data were processed and unit cell constants were refined with the SAINT program utilizing 2482 reflections [22]. Absorption corrections were rejected because they did not improve the quality of data. The structure of **1** was determined successfully in the orthorhombic space group *Pbca* (no. 61). Compound **2** was found to be in the triclinic cell system and was solved in space group $P\bar{1}$ (no. 2). There are three independent molecules in the asymmetric unit. Compounds **3** and **4** were assigned to the space group $P2_1/c$ (no. 14) based on systematic absences. Relevant crystallographic parameters for **1**–**4** are given in Table 1. Structure solution and refinement was carried out using SHELXS-86 [23] and SHELXL-93 [24]. No corrections were made for secondary extinction. Absorption corrections made on **1**, **3**, and **4**, using semiempirical Psi scans, resulted in little or no improvement of the structures. No absorption correction was made on **2**. The solutions for **1**–**4** were obtained using direct methods which allowed for assignment of the selenium atoms. The carbon atoms were located in subsequent refinement cycles. The hydrogen atom positions were calculated and riding on the carbon atoms to which they were bound ($d_{CH} = 0.96$ Å).

4. Results and discussion

The two diorganoselenides, (2-MeBz)$_2$Se (**1**) and MeMes*Se (**2**) and the diorganodiselinides Mes_2Se_2 (**3**) and $Mes^*_2Se_2$ (**4**) were prepared as described. Com-

Table 1
Selected experimental parameters for the X-ray diffraction studies of (2-MeBz)$_2$Se (**1**), MeMes*Se (**2**), Mes_2Se_2 (**3**) and $Mes^*_2Se_2$ (**4**)

Compound	**1**	**2**	**3**	**4**
Formula	$C_{16}H_{18}Se$	$C_{19}H_{32}Se$	$C_{18}H_{22}Se_2$	$C_{36}H_{58}Se_2$
Formula weight	289.26	339.41	396.28	648.74
Crystal structure	Orthorhombic	Triclinic	Monoclinic	Monoclinic
Space group	*Pbca* (no. 61)	$P\bar{1}$ (no. 2)	$P2(1)/c$ (no. 14)	$P2(1)/c$ (no. 14)
a (Å)	13.944(10)	5.9443(5)	6.3330(10)	11.359(5)
b (Å)	13.944(10)	18.665(2)	18.370(4)	10.520(8)
c (Å)	14.30(2)	26.372(3)	15.122(3)	30.22(2)
α (°)	90	99.393(2)	90	90
β (°)	90	90.890(2)	97.42(3)	98.94(4)
γ (°)	90	92.703	90	90
V (Å^3)	2779(4)	2882.7(5)	1744.5(6)	3567(4)
Z	8	6	4	4
$D_{calc.}$ (g cm^{-3})	1.383	1.173	1.509	1.208
F(000)	1184	1080	792	1368
R_1 ($I>2\sigma I$)	0.0652	0.0778	0.0437	0.0608
wR_2 ($I>2\sigma I$)	0.1068	0.1500	0.0964	0.0886
R_1 (all data)	0.182	0.230	0.0638	0.1425
wR_2 (all data)	0.141	0.218	0.1046	0.1077
Goodness-of-fit	0.898	0.922	1.071	0.888

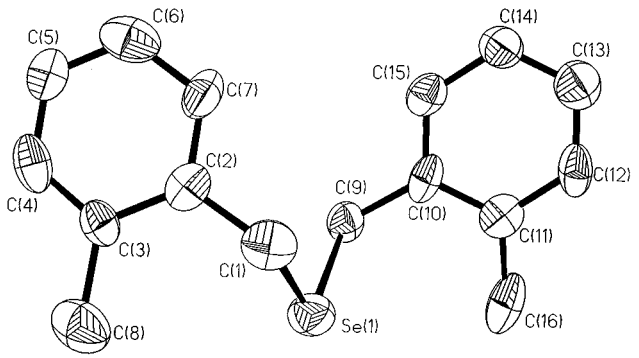

Fig. 1. Thermal ellipsoid diagram (50% thermal ellipsoids) of (2-MeBz)$_2$Se (**1**). Hydrogen atoms have been omitted for clarity.

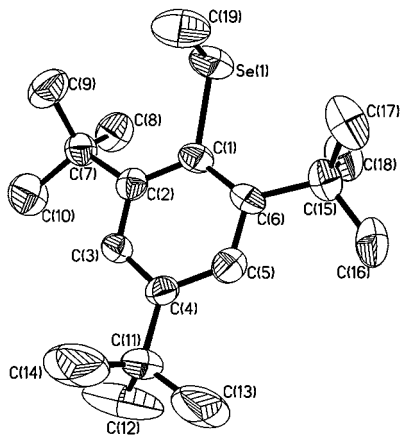

Fig. 2. Thermal ellipsoid diagram (50% thermal ellipsoids) of MeMes*Se (**2**). Hydrogen atoms have been omitted for clarity.

Table 2
Selected bond distances (Å) and angles (°) for (2-MeBz)$_2$Se (**1**), and MeMes*Se (**2**)

(2-MeBz)$_2$Se (**1**)		MeMes*Se (**2**)	
Bond length			
Se(1)–C(9)	1.949(10)	Se(1)–C(1)	1.949(7)
Se(1)–C(1)	1.983(11)	Se(1)–C(19)	1.955(8)
Bond angle			
C(9)–Se(1)–C(1)	98.6(4)	C(1)–Se–C(19)	96.3(3)

pound **1** is the first dialkyl selenide without a ketone or other functional group attached at the C(2) position, **2** is a simple selenide with one substituent, the very bulky super mesityl group. Both were characterized by X-ray diffraction. Diagrams of **1** and **2** with atom labeling schemes are shown in Figs. 1 and 2. Selected bond distances and angles are given in Table 2. The observed bond distances and angles are similar to those reported for other aryl and alkyl selenides [25,26].

Compounds **3** and **4** have similar substituents bound to the Se–Se backbone with **4** again containing the very bulky Mes* group. Their structures have been determined and are shown in Figs. 3 and 4 with selected bond distances and bond angles given in Table 3. The Se–Se and Se–C bond distances fall within the expected range.

It has been reported that diselenides relieve steric strain by increasing the C–Se–Se–C dihedral angle rather than by increasing the Se–Se and Se–C bond lengths [3]. The current studies support this with the C–Se–Se–C dihedral angle in **3** as being 83.5°, which is well within the range of 73–87° reported for many of the less bulky diselenides, while that of **4**, 93.3°, lies between these and the more sterically hindered diselenides such as $[(Me_3Si)_3C]_2Se_2$, $(2,6\text{-}Mes_2C_6H_3)_2Se_2$, and $[(t\text{-}Bu)_2CH]_2Se_2$ which have dihedral angles ranging from 102.4 to 180° (see Table 4).

Further support for this hypothesis comes from a comparison of **3** with bis-(2,4,6-tris-trifluoromethylphenyl)-diselenide [4], which shows the effects of substituting F atoms for H atoms on the methyl groups in the 2, 4 and 6 positions. This leads to an increase in the dihedral angle from 83.5° for **3** to 104° for the fluorinated derivative. This increase in dihedral angle appears to be due to the increase in steric interactions rather than to a change in the electronic proper-

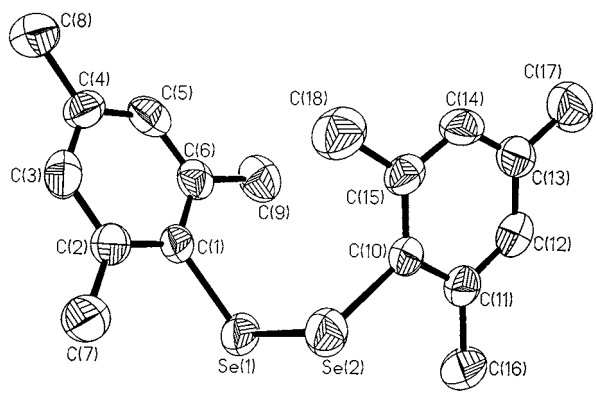

Fig. 3. Thermal ellipsoid diagram (50% thermal ellipsoids) of Mes_2Se_2 (**3**). Hydrogen atoms have been omitted for clarity.

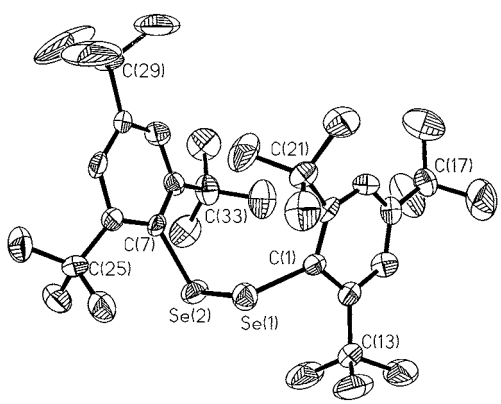

Fig. 4. Thermal ellipsoid diagram (50% thermal ellipsoids) of $Mes^*_2Se_2$ (**4**). Hydrogen atoms have been omitted for clarity.

Table 3
Selected bond distances (Å) and angles (°) for Mes_2Se_2 (**3**) and $Mes^*_2Se_2$ (**4**)

Mes_2Se_2 (**3**)		$Mes^*_2Se_2$ (**4**)	
Bond length			
Se(1)–C(1)	1.925(6)	Se(1)–C(1)	1.932(7)
Se(1)–Se(2)	2.328(1)	Se(1)–Se(2)	2.345(2)
Se(2)–C(10)	1.929(6)	Se(2)–C(7)	1.954(7)
Bond angle			
C(1)–Se(1)–Se(2)	101.1(2)	C(1)–Se(1)–Se(2)	103.1(2)
C(10)–Se(2)–Se(1)	100.5(2)	C(7)–Se(2)–Se(1)	102.8(2)
C(2)–C(1)–Se(1)	119.6(5)	C(6)–C(1)–Se(1)	120.3(6)
C(6)–C(1)–Se(1)	119.1(5)	C(2)–C(1)–Se(1)	120.7(6)
C(15)–C(10)–Se(2)	119.9(5)	C(12)–C(7)–Se(2)	119.6(6)
C(11)–C(10)–Se(2)	118.9(5)	C(8)–C(7)–Se(2)	118.8(6)
C(1)–Se(1)–Se(2)–C(10)	83.4(3)	C(1)–Se(1)–Se(2)–C(7)	93.3(3)
Se(1)–C(1)–C(2)–C(7)	2.2(8)	Se(1)–C(1)–C(2)–C(13)	23.0(10)
Se(1)–C(1)–C(6)–C(9)	1.4(8)	Se(1)–C(1)–C(6)–C(21)	22.2(10)
Se(2)–C(10)–C(11)–C(16)	3.8(8)	Se(2)–C(7)–C(8)–C(25)	25.2(10)
Se(2)–C(10)–C(15)–C(18)	2.9(8)	Se(2)–C(7)–C(12)–C(33)	21.3(10)

ties of the compound. The electronic effects appear to have the opposite effect as shown in the comparison of diphenyl diselenide and bis(perfluorophenyl) diselenide, which shows a decrease in the dihedral angle from 82 to 75.3° [9,27]. This may be the result of the fluorinated aromatic ring removing electron density from the lone pairs on the selenium atoms, allowing the system to adopt a more eclipsed configuration (Scheme 1).

The structure of **3** can also be compared to the tellurium analog [28]. The ditelluride has a dihedral angle of 93.9° compared to 83.5° for **3**. In general, the dihedral angle in a given species increases as the chalcogen is changed from S to Se to Te.

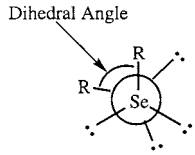

Scheme 1. View down the Se–Se bond of a typical diselenide.

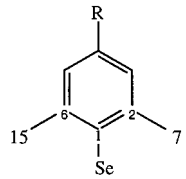

Scheme 2. Se–C–C–C torsion angles Se–1–2–7 and Se–1–6–6.

When the bulky substituent Mes* is present, the structures are distorted. In **2**, the Se–C(1)–C(6)–C(15) and the Se–C(1)–C(2)–C(7) torsion angles are 21.9 and 21.0°, and the corresponding torsion angles in **4** are 18.8 and 19° (see Scheme 2). This indicates that there is substantial steric interaction resulting in the Se atom and *ortho* tertiary butyl groups being bent out of the plane of the phenyl ring in opposite directions.

Another way to describe this is to note that the *t*-butyl groups in the *ortho* positions are bent away from the ring plane by nearly 10° while the *para* *t*-butyl group is a less severe 4° out of the plane. These distortions are seen graphically in Scheme 3. In all of the other structurally characterized aromatic diselenides with *ortho* groups, this angle ranges from 0 to 7°. Even greater distortions are found in the structure of $Mes^*_2Te_2$ with the Te atoms and the *t*-butyl groups bent out of the plane of the phenyl ring, giving Te–C–C–C torsion angles of 29.0 and 26.2°.

Table 4
C–Se–Se–C torsion angle and Se–Se bond distance in selected diselenides

Compound	Torsion angle (°)	Se–Se bond distance (Å)	Reference
$[(Me_3Si)_3C]_2Se_2$	180.0	2.387	[1]
(2,6-$Mes_2Ph)_2Se_2$	128.2	2.339	[2]
$[(t\text{-}Bu)_2CH]_2Se_2$	112.0	2.315	[3]
[2,4,6-$(CF_3)_3Ph]_2Se_2$	104.0	2.310	[4]
(2-$NO_2Ph)_2Se_2$	102.4	2.330	[5]
(*p*-$CH_3Ph)Se_2$	99.7	2.328	[6]
$Mes^*_2Se_2$	93.3	2.347	This work
(*p*-$NO_2Ph)Se_2$	87.8	2.302	[7]
Mes_2Se_2	83.5	2.330	This work
Ph_2Se_2	82.5	2.287	[9]
$(Ph_2CH)_2Se_2$	82.0	2.285	[10]
{2,6-[1-(EtO)Et]$_2$Ph}$_2Se_2$	77.2	2.328	[34]
(*p*-ClPh)$_2Se_2$	74.2	2.332	[8]
$(F_5C_6)_2Se_2$	73.6	2.319	[27]
(2,6-*i*-$Pr_2Ph)_2Se_2.I_2$	73.0	2.354	[11]

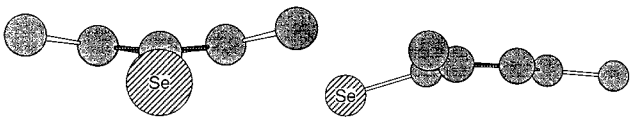

Scheme 3. Chem 3D drawing of $MeMes^*_2Se$ (**2**), viewed along phenyl ring edge.

4.1. NMR studies

It has been shown that some hindered disulfides, diselenides [13], and ditellurides [29] exhibit slow rotation about the E–E and/or the E–C bonds which can be seen as the alkyl groups in the 2 and 6 positions are locked in a conformation where they are non-equivalent. Kessler and Rundel [13] have discussed this in some detail and have reported thermodynamic and kinetic parameters for several systems, including **4**, and du Mont et al., have discussed this for the analogous ditelluride [29].

With the availability of a high-field NMR spectrometer, we decided to reexamine this process and studied both **3** and **4** by ^{1}H-, ^{13}C-, ^{77}Se-, and variable-temperature NMR spectroscopy. Compound **3** shows the predicted NMR patterns in the ^{1}H and ^{13}C spectra and a ^{77}Se signal at 368 ppm, consistent with other diselenides, but does not show any evidence for slowing the rotational processes at -40°C, indicating that the barriers to rotation about the Se–Se and Se–C bonds in **3** are relatively low and that the mesityl group is not sufficiently bulky to hinder rotation in this molecule.

In **4**, the ^{13}C- and ^{77}Se-NMR spectra show the expected patterns and are reported in Section 2. Fig. 5 shows a stacked plot of the 500 MHz ^{1}H-NMR spectrum of the *t*-butyl region as a function of temperature. The spectrum at 55°C represents the fast exchange limit and shows the pattern expected for an Mes* group. The slow exchange limit is best seen in the -40°C spectrum where the *ortho t*-butyl groups become non-equivalent; similarly, the *meta* ring protons are non-equivalent at this temperature. In the intermediate region, the spectrum exhibits the normal behavior for an exchanging system.

The mechanism proposed for this process has been described by Kessler and Rundel [13] and is shown in Scheme 4. It consists of two rotational processes, one about the Se–Se bond and the second about the Se–C bond. The barrier measured is for the rate-determining process. Thermodynamic and activation energy parameters were calculated from variable-temperature NMR data using three different methods: (1) from the coalescence temperature [13]; (2) calculation of the rate parameters from the half width [30]; and (3) by a complete line shape analysis using the WinDNMR program [31].

The simplest approach is to use the coalescence temperature. By performing the experiment on both 300 and 500 MHz spectrometers, using the coalescence of

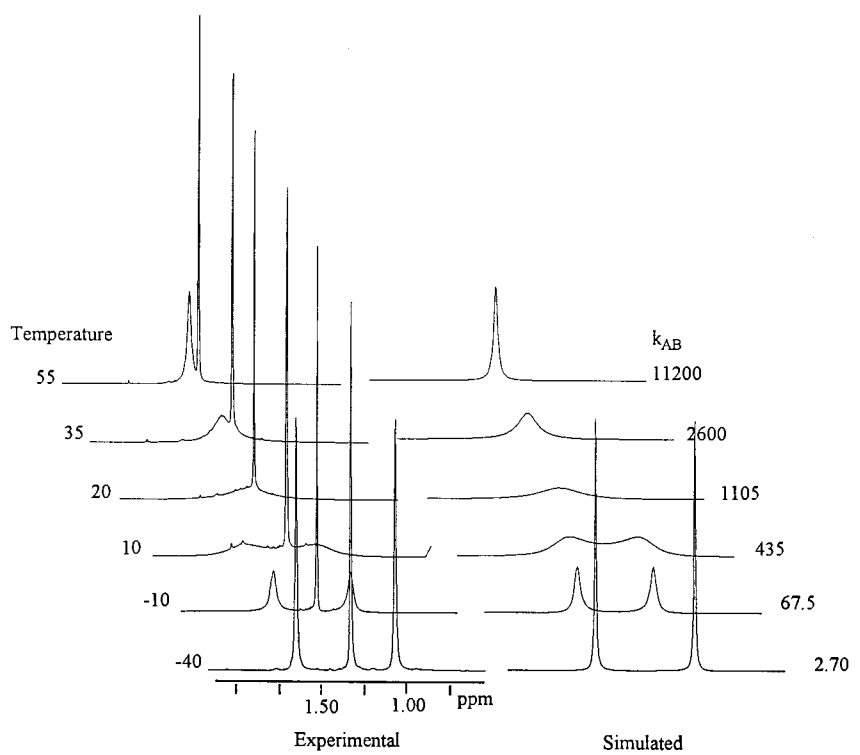

Fig. 5. A stacked plot showing the change in line shape of the 500 MHz ^{1}H-NMR spectrum as a function of temperature (left) and the simulated spectrum using a two-site model (right).

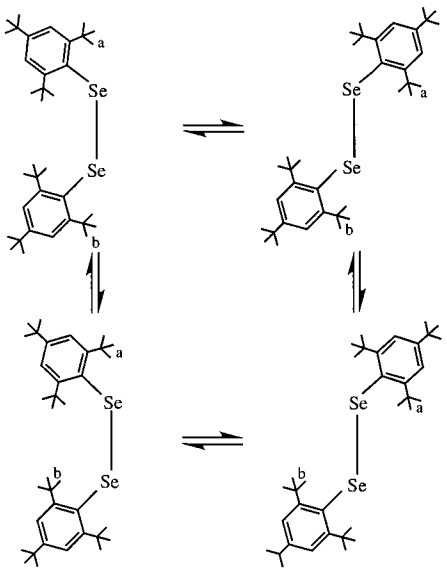

Scheme 4.

the *meta* proton and the *t*-butyl groups, we were able to obtain rate constants at four different temperatures.

The second method used to estimate the rate constant is from the half width ($v_{1/2}$) of the lines associated with the exchange process. To improve the results from this method, line widths were measured using a deconvolution program which provided a best fit simulation of the desired peak. The average of the two line widths were used in the calculation of the rate constant. This approach is limited to the slow exchange region where the two exchanging sites give rise to separate resonances that lie between 10 and -30°C for this system.

The third method used was to simulate the variable-temperature NMR spectra using the program WinDNMR [31]. The advantage of this technique is that rate constants can be obtained over a wider temperature range, including both the slow and fast regions. Simulated spectra were obtained using a two-site exchange model (A and B) representing the two observed *ortho* signals. The rate constant $k_{ab} + k_{ba}$ was varied in order to match the experimental spectrum. Halving this value provided the rate constant k_{ab} for the process under investigation. Non-exchange line widths of 0.5 Hz were used at temperatures above -30°C, while for temperatures of -30°C and below it was necessary to increase

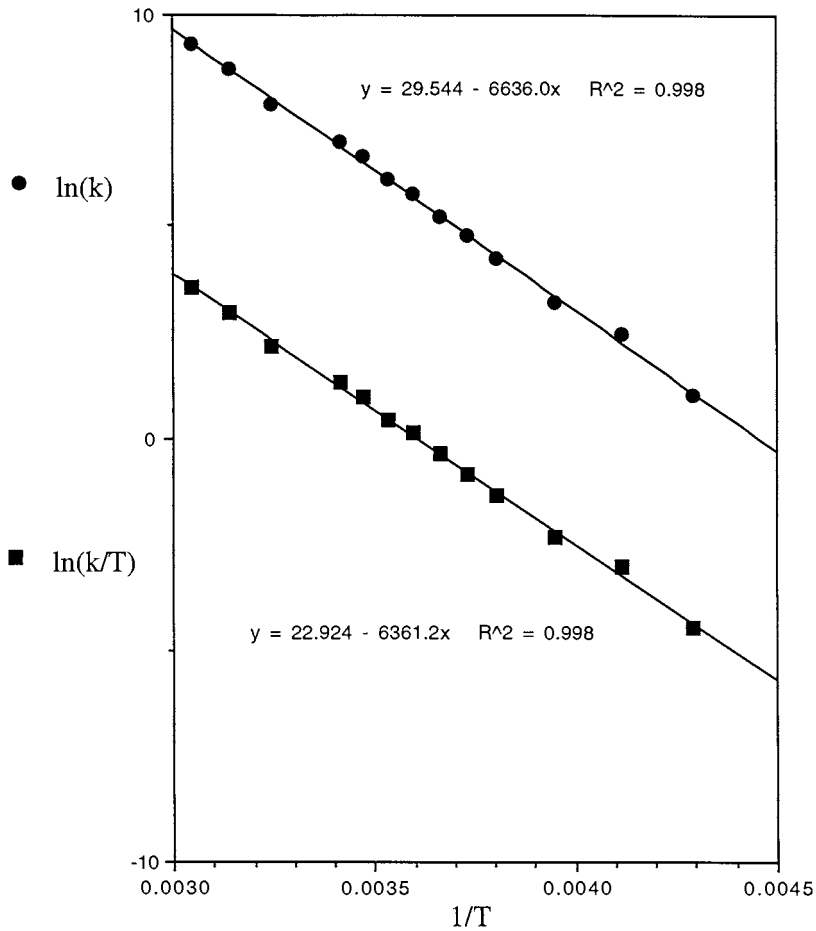

Fig. 6. Arrhenius and Eyring plots for the rotational process observed in $Mes^*_2Se_2$ (**4**). The lifetimes were obtained from the complete line shape analysis.

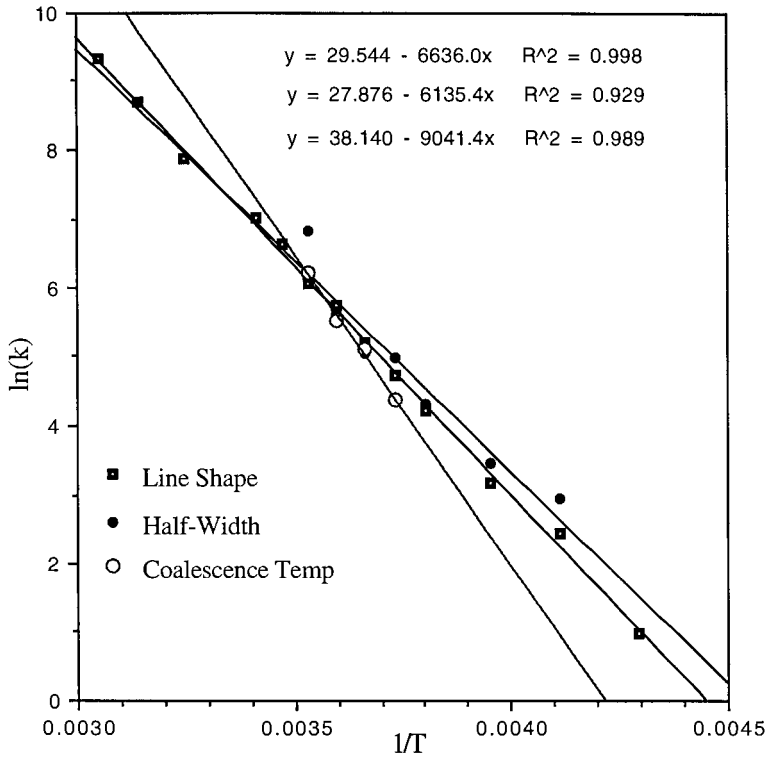

Fig. 7. Arrhenius plots for the rotational process illustrating the differences between the coalescence temperature measurements, the $v_{1/2}$ approximation, and the complete line shape analysis.

the non-exchange line width to account for line broadening due to sample viscosity.

All three methods give information about the kinetics for the processes involved. With the data available, both Arrhenius and Eyring plots can be generated. These are both shown in Fig. 6, using the rate constants obtained from the full line shape analysis.

Comparison of the Arrhenius plots obtained from the three methods of analysis is shown in Fig. 7. The results from the half-width approximation and the complete line shape analysis are in relatively good agreement, while the results for these parameters from the coalescence approximation deviate sharply. It can be seen from Table 5 that the most uncertainty is found in the entropy parameter where there is little agreement between the three methods. The activation parameters obtained from this experimental study are comparable to the energy barriers calculated for the rotation about the Se–Se bond in Me_2Se_2 [32], but the hindered rotation can only be observed when both Se–Se and C–Se bond rotations are slow. From the data available, we cannot determine which process is rate determining, but it is clear that the best method is to use the complete line shape analysis where possible for both the kinetic and thermodynamic parameters.

The chemical shift differences observed for the *t*-butyl groups at low temperature arise from their proximity to the shielding or deshielding regions of the phenyl ring. The distance separating the *t*-butyl group from the ring can be estimated roughly from the chemical shift difference between the *t*-butyl group opposite the benzene ring and the unaffected *t*-butyl group [33] and compared to that in the solid state. The difference in chemical shift for the *ortho t*-butyl groups at -60°C is 0.60 ppm while for the *meta* protons, which are out of the shielding region, the difference is 0.20 ppm. Based on the change in chemical shift, it is estimated that the distance between the aromatic group and the methyl protons of the *t*-butyl group is greater than 4.4 Å in solution at -60°C. In the solid state this distance is on the order of 3.5 Å. It should be noted that the shift in the NMR signal will be the average of the three methyl groups of the *t*-butyl moiety due to the free rotation about the C–C bond in solution. In the solid state structure this average distance is 4.7 Å. Therefore an average distance of 4.4 Å above the phenyl ring is a reasonable result and shows that the structure in solution at low temperature is quite similar to that in the solid state.

5. Supplementary material

Complete crystal data, bond distances and angles, anisotropic displacement parameters for all non-hydrogen atoms, atomic coordinates and isotropic thermal

Table 5
Kinetic and thermodynamic parameters for the three methods of analysis of $Mes^{*}_{2}Se_{2}$ (**4**)

Analysis method	Coalescence	Half-width	WinDNMR
Number data points	4	7	13
$\Delta H^{\ddagger}$ (kJ mol^{-1})	73	48.8	52.9
$\Delta S^{\ddagger}$ (J mol^{-1} °$^{-1}$)	65	20.4	6.92
$\Delta G^{\ddagger}$ at +50°C (kJ mol^{-1})	52	42.2	50.7
$\Delta G^{\ddagger}$ at 0°C (kJ mol^{-1})	55	43.2	51.0
$\Delta G^{\ddagger}$ at −50°C (kJ mol^{-1})	58	44.2	51.3
E_a (kJ mol^{-1})	76	51.0	55.2

parameters for all non-hydrogen atoms, and hydrogen atom coordinates and isotropic displacement parameters have been deposited with the Cambridge Crystallographic Data Center (CCDC). These data can be obtained free of charge from the Director, Cambridge Crystallographic Data Center, 12 Union Road, Cambridge, CB2 1EZ, UK, citing the deposition numbers 124682, 124683, 124684 and 124685 for compounds **1**, **2**, **3** and **4**, respectively, the authors and the reference (e-mail: deposit@ccdc.cam.ac.uk).

Acknowledgements

Acknowledgment is made to the donors of the Petroleum Research Fund administered by the American Chemical Society for the support of this research.

References

[1] I. Wagner, W.-W. du Mont, S. Pohl, W. Saak, Chem. Ber. 123 (1990) 2325.
[2] J.J. Ellison, K. Ruhlandt-Senge, H.H. Hope, P.P. Power, Inorg. Chem. 34 (1995) 49.
[3] T.G. Back, P.W. Codding, Can. J. Chem. 61 (1983) 2749.
[4] N. Bertel, H.W. Roesky, F.T. Edelmann, M. Noltemeyer, H.G. Schmidt, Z. Anorg. Allg. Chem. 586 (1990) 7.
[5] E.A. Meyers, R.A. Zingaro, N.L.M. Dereu, Z. Kristallogr. 210 (1995) 305.
[6] G. Van den Bossche, M.R. Spirlet, O. Dideberg, L. Dupont, Acta Crystallogr. C (Cryst. Struc. Commun.) 40 (1984) 1979.
[7] G.D. Morris, F.W.B. Einstein, Acta Crystallogr. C (Cryst. Struc. Commun.) 42 (1986) 1433.
[8] F.H. Kruse, R.E. Marsh, J.D. McCullough, Acta Crystallogr. 10 (1957) 201.
[9] R. Marsh, Acta Crystallogr. 5 (1952) 458.
[10] H.T. Palmer, R.A. Palmer, Acta Crystallogr. Sect. B 25 (1969) 1090.
[11] W.-W. du Mont, A. Martens, S. Pohl, W. Saak, Inorg. Chem. 29 (1990) 4847.
[12] K.-S. Tan, A.P. Arnold, D.L. Rabenstein, Can. J. Chem. 66 (1988) 54.
[13] H. Kessler, W. Rundel, Chem. Ber. 101 (1968) 3350.
[14] D.F. Shriver, M.A. Drezdzon, The Manipulation of Air-Sensitive Compounds, Wiley, New York, 1986.
[15] D.E. Pearson, M.G. Frazer, V.S. Frazer, L.C. Washburn, Synthesis (1976) 621.
[16] W. Rundel, Chem. Ber. 101 (1968) 2956.
[17] M. Bochmann, K.J. Webb, M.B. Hursthouse, M. Mazid, J. Chem. Soc. Dalton Trans. (1991) 2317.
[18] D.G. Foster, in: E.C. Horning (Ed.), Selenophenol (Benzeneselenol), vol. 3, 1955, pp. 771–773.
[19] H.J. Reich, M.L. Cohen, P.S. Clark, in: W.E Noland (Ed.), Reagents for the Synthesis of Organoselenium Compounds: Diphenyl Diselenide and Benzene-selenyl Chloride, vol. 6, Wiley, New York, 1988, pp. 533.
[20] W.-W. du Mont, S. Kubiniok, L. Lange, S. Pohl, W. Saak, I. Wagner, Chem. Ber. 124 (1991) 1315.
[21] SHELXTL PC, Siemens Analytical X-Ray Instruments, Inc. Madison, WI, 1990.
[22] SMART/SAINT, Siemens Analytical X-Ray Instruments, Inc. Madison, WI, 1996.
[23] G.M. Sheldrick, SHELX-86, University of Göttingen, Göttingen, FRG, 1986.
[24] G.M. Sheldrick, SHELXL-93, University of Göttingen, Göttingen, FRG, 1993.
[25] G.V.N. Appa Rao, M. Seshasayee, G. Aravamudan, S. Sowrirajan, Acta Crystallogr. C39 (1983) 620.
[26] D.D. Dexter, Acta Crystallogr. B28 (1972) 49.
[27] C.M. Woodard, D.S. Brown, J.D. Lee, A.G. Massey, J. Organomet. Chem. 121 (1976) 333.
[28] A. Edelmann, S. Brooker, N. Bertel, M. Noltemeyer, H.W. Roesky, G. Sheldrick, F.T. Edelmann, Z. Naturforsch. Teil B. 47 (1992) 305.
[29] W.-W. du Mont, L. Lange, H.H. Karsch, K. Peters, E.M. Peters, H.G. von Schnering, Chem. Ber. 121 (1988) 11.
[30] E.D. Becker, Exchange Processes: Dynamic NMR, Academic, New York, 1980, pp. 240–252.
[31] H.J. Reich, WinDNMR: Dynamic NMR Spectra for Windows, J. Chem. Educ. Softw. 30 (1996) 27.
[32] V. Renugopalakrishnan, R. Walter, J. Am. Chem. Soc. 106 (1984) 3413.
[33] C.E. Johnson Jr., F.A. Bovey, J. Chem. Phys. 29 (1958) 1012.
[34] R. Deziel, S. Goulet, L. Grenier, J. Bordeleau, J. Bernier, J. Org. Chem. 58 (1993) 3619.